JOURNAL OF GEOPHYSICAL RESEARCH, VOL. 106, NO. A5, PAGES 8465–8476, MAY 1, 2001

Auroral plasma turbulence and the cause of auroral kilometric radiation fine structure

Raymond Pottelette

Centre des Études Terrestres et Planétaires, Saint-Maur-des-Fossés, France

Rudolf A. Treumann[1]

Centre for Interdisciplinary Plasma Science, Max-Planck-Institute for extraterrestrial Physics, Garching Germany

Matthieu Berthomier[2]

Centre des Études Terrestres et Planétaires, Saint-Maur-des-Fossés, France

Abstract. Electron holes excited in the auroral kilometric radiation (AKR) source region in presence of a very dilute cool electron background are interpreted as causing the observed fine structure in AKR radiation. Using high time and frequency resolution measurements of the FAST wave tracker, we demonstrate that a substantial part of the AKR emission consists of a large number of elementary radiation events that we interpret as traveling electron holes that may have resulted from the nonlinear evolution of electron acoustic waves and have the properties of Bernstein-Green-Kruskal modes. Estimates of the propagation velocity of these structures are in good agreement with theory. Power estimates show that each elementary radiation event may contribute $\simeq 10^{3-4}$ W of power to AKR implying that a moderately large number of elementary radiators is required to reproduce the total AKR emission. The elementary radiation structures are sometimes reflected from the acceleration potential or become trapped in larger structures like ion acoustic waves or ion holes. The observations indicate that the radiation efficiency is highest at the turning point where the velocity of the elementary radiators with respect to the reflector system vanishes. Monitoring the time variation of the frequency drift of the elementary radiators allows to qualitatively infer about the mesoscale motion of the AKR source region and the spatial extension of the mesoscale field-aligned electric potential drops.

1. Introduction

Pritchett [1984], *Pritchett et al.* [1999], and *Winglee and Pritchett* [1986] first proposed that auroral kilometric radiation (AKR) is most effectively generated by the electron-cyclotron maser mechanism acting on a so-called horseshoe electron distribution. It has theoretically been predicted by *Chiu and Schulz* [1978] that such distributions may evolve in the interaction of a mirroring electron beam with a field-aligned electric potential and has been subsequently observed by *Delory et al.* [1998]. The prediction of generation of AKR by these distributions [*Pritchett and Strangeway*, 1985] has been confirmed by observations from the FAST spacecraft [*Carlson et al.*, 1998a] of both particles and waves in the AKR source region [*Ergun et al.*, 1998a, 1998b; *Strangeway et al.*, 1998, 2000].

It is crucial for this theory that the plasma be very dilute such that the ratio $f_{pe}^2/f_{ce}^2 \ll 1$ of electron plasma to cyclotron frequencies is sufficiently small in order to prevent wave damping. In addition, the horseshoe distribution allows for an extended region in phase space where the perpendicular phase space gradient $\partial f_e/\partial v_\perp > 0$ of the electron velocity distribution is positive. This property strongly increases the growth rate over that of the ordinary loss-cone electron-cyclotron maser mechanism of *Wu and Lee* [1979]. Such a distribution also possesses a positive gradient $\partial f_e/\partial v_{||} > 0$ in the parallel direction which in the presence of a however weak cool background plasma density excites electron acoustic waves [*Winglee and Pritchett*, 1986]. The electron-cyclotron maser and electron hole instabilities therefore do not develop independently but share the available free energy stored in the particle distribution.

In this paper we present evidence for the presence of nonlinear electron acoustic waves or electron holes in the AKR source region. At the edges of the acceleration region, electron acoustic waves are excited very strongly reaching amplitudes of up to $E \approx 1\ \mathrm{V\,m^{-1}}$ [*Pottelette et al.*, 1999]. Using high-resolution wave tracker data of FAST during AKR we investigate the properties of the frequency and time fine structure of AKR and demonstrate that a considerable frac-

[1]Also at International Space Science Institute, Bern, Switzerland.

[2]Now at Space Sciences Laboratory, University of California, Berkeley, California.

Paper number 2000JA000098.
0148-0227/01/2000JA000098$09.00

tion of the emission consists of a large number of elementary radiation events which we interpret as the signature of the interaction of localized electron acoustic waves (electron holes) with the horseshoe electron particle distribution. The large-scale dynamics of the AKR source region may be inferred from the spectral drift of the elementary emissions.

Since our observations have been performed in the upward current region, the issue is somewhat controversial. Previously, electron holes have been reported mainly from the downward current region in the auroral zone [*Carlson et al.*, 1998b; *Ergun et al.*, 1998a] where large numbers of electron holes have been detected by the FAST spacecraft. Observations of similar structures in the upward current region are sparse though not absent [*Ergun et al.*, 1999]. In all those cases, indication of the existence of such holes is derived from the 32-kHz electric wave form. Because of lack of time resolution it is much more difficult to infer about the electron distribution function in the electron holes. A few such measurements have been collected by *Carlson et al.* [1998b] and by *Ergun et al.* [1999] for the downward current region only. We are therefore faced with the problem of the apparent rarity of electron holes in the upward current AKR source region.

In the following we will take the observation of the distinct AKR fine structure as evidence for the presence of large numbers of electrons holes in the boundaries of the upward current region. Fine structure in AKR had already been observed earlier for instance by *Gurnett and Anderson* [1981] though not with the now available time and frequency resolution. In our previous paper [*Pottelette et al.*, 1999] we argued that the main source of plasma turbulence is just located at the boundaries of the auroral density cavity where very strong broadband noise is observed regularly. There is still an appreciable amount of cold plasma at this place which is needed to excite the electron acoustic turbulence. Because of the lack of cold plasma in the center of the acceleration region, electron acoustic turbulence will be weak in this region. So one does not expect that electron holes will be generated here.

The broadband noise at the edges of the AKR source region, on the other hand, may consist of a large number of electron holes [*Dubouloz et al.*, 1993; *Berthomier*, 2000]. These are however difficult to resolve in the spectra as well as in the electron distribution function. In the high time-resolved wave spectra they appear as highly localized and very intense (up to several $100\,\mathrm{mV\,m^{-1}}$) electrostatic features in the kHz range [*Pottelette et al.*, 1999, Figure 2] of very narrow transverse spatial extension of down to some tens of meters. Thus we claim that the AKR fine structure is generated at the boundaries of the ionospheric plasma cavities and reflects the properties of the turbulence in this region.

2. Observations

VLF wave measurements [*Strangeway et al.*, 1998] in the upward current density cavities which serve as the AKR source have provided support for the hot (>1 keV) electron component to be much in excess of cold background electrons. The accelerated ion beam observed in this region provides the neutralizing background. These properties indicate that the plasma has undergone acceleration in a mesoscale field-aligned electric potential which lifts the electron distribution, backscatters electrons, and generates the cold ion beam along the magnetic field. The combined action of the electric potential and the mirror force thus leads to spreading of the original parallel electron beam into a distribution that assumes an incomplete ring or horseshoe-like shape in phase space [*Ergun et al.*, 1998a, 1998b].

2.1. AKR Source Region

Plate 1 shows a sequence of FAST wave and particle measurements in the AKR source region obtained on January 30, 1997, at ~2200 MLT (orbit 1750). The spacecraft was at an invariant latitude of ~68° and was traveling poleward, near apogee, at an altitude of 4300 km. The AKR event shown took place in the upward current region. Figures 1a and 1b display the respective omnidirectional ion and electron energy fluxes versus energy and time for the same time period. Plates 1c and 1d give the electric power spectral densities at high (4 kHz to ~600 kHz) and low frequencies (32 Hz to 16 kHz), respectively.

Since the data have been described in a different context by *Pottelette et al.* [1999], we here mention only the main features of the event. The edge of the AKR source region manifests itself as the location of steep increase of the ion energy and upgoing ion beam formation caused by the auroral acceleration process. FAST entered this region at ~0616:33 UT (Plate 1a). Here the cold electron density, however small, is still significant. Afterward, the spacecraft stayed for ~24 s inside the AKR source region (Plate 1c). The electromagnetic AKR emission is generated at and also slightly below the local nonrelativistic electron-cyclotron frequency f_{ce} at ~340 kHz (dark line in the plate), which in the current understanding of the emission process is an indication of the relativistic modification of the maser emission which causes the X-mode cutoff to be below the nonrelativistic electron-cyclotron frequency. The modulation of the AKR shows the radiation to be in the $X(Z)$ mode with the Z mode appearing as the weak radiation extending well below the cyclotron frequency down to 200 kHz.

In the low-frequency part of the spectrum (Plate 1d) the source region exhibits weak O-mode radiation identified from its opposite polarization which is out of phase with that of the $X(Z)$-mode in Plate 1c, and the VLF emission. The O-mode emission weakens close to the total plasma frequency, while the VLF emission is cutoff at this place. The latter gives an estimate for the hot plasma density, which has been found to be in good agreement with the particle observations under the assumption of a very dilute cold electron background [*Pottelette et al.*, 1999]. The density of this hot population was $n_h \approx 0.3\,\mathrm{cm^{-3}}$. The O mode has a significant magnetic component. Its cut-off provides a measurement of the total electron density. The gap between the two cutoffs in Plate 1d thus gives an indication of the contribu-

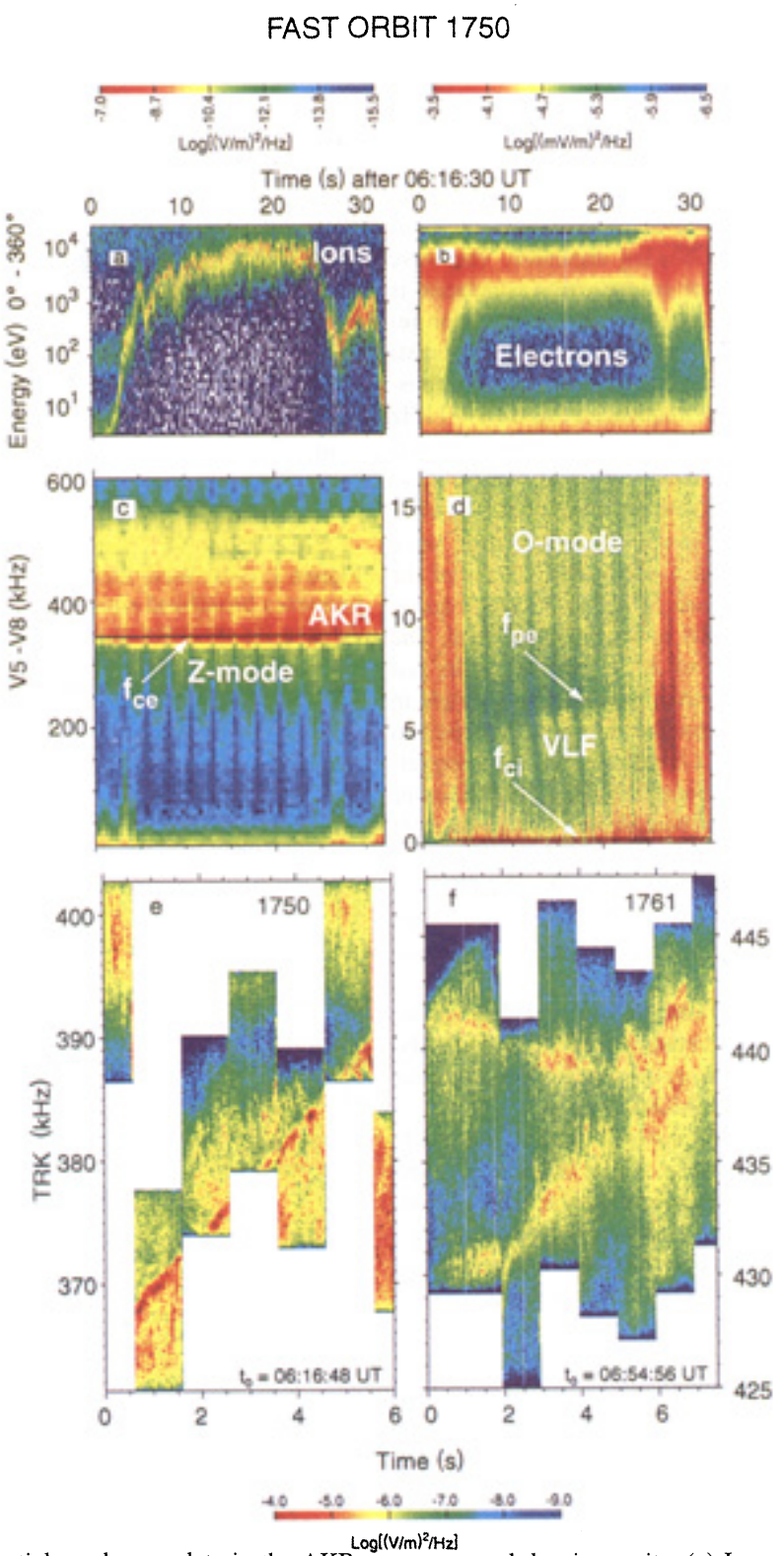

Plate 1. Fast particle and wave data in the AKR source auroral density cavity. (a) Ion and (b) electron energy spectra for same time interval of orbit 1750. (c) HF wave spectrogram showing transversely polarized AKR emission at f_{ce} (dark line at ~340 kHz) in X and below in Z mode and VLF waves. (d) VLF wave spectrogram showing parallel polarized O mode, electron acoustic and ion cyclotron (dark line at ~200 Hz) waves. At base of AKR source broadband electron acoustic waves appear. (e) Wave tracker observations during the indicated zoomed time interval of orbit 1750, showing the steady drifting in frequency emission feature embedded into a large number of fast drifting narrow band elementary emitters. (f) Similar tracker data taken during orbit 1761.

tion of the cold plasma density. Clearly, its density is not constant across the cavity. Unfortunately, owing to propagation effects and weakening the O-mode cutoff is not as well defined. Estimating a $\simeq 1$ kHz bandwidth of the gap one finds a tentative value of $n_c \approx 0.01\,\mathrm{cm}^{-3}$ for the remaining cold background plasma density.

A more precise estimate than the O-mode cutoff yields can be obtained from the following argument. The wave mode characterizing the minor cold electron population is the electron acoustic mode. In the parallel acceleration region it manifests itself as the transient broadband wave bursts [*Pottelette et al.*, 1999] seen in Plate 1d. Such transient emissions occur in large number at frequencies less than ~ 1 kHz inside the AKR source region. According to the theoretical prediction [*Winglee and Pritchett*, 1986] the weak electrostatic emissions indicate the presence of a minor cold electron component, if they are in the electron acoustic wave mode. Figure 1 on its left-hand side shows 100 ms of the electric field signal during one of the electrostatic bursts when the antenna was parallel to the magnetic field. The burst has typical amplitudes of $E \approx 10\,\mathrm{mV\,m}^{-1}$. Its fast Fourier transform (FFT)-spectrum is plotted on the right in Figure 1. This spectrum is broadband, typical for electron acoustic turbulence, showing a cutoff at ~800 Hz. Interpreting this cutoff as the cold plasma frequency f_{pc} [*Dubouloz et al.*, 1993], one finds that the cold plasma density amounts to $n_c \approx 0.008\,\mathrm{cm}^{-3}$, corresponding roughly to the 3% of the total plasma density estimated above from the O-mode cutoff. This confirms the previous assertion [*Strangeway et al.*, 1998] of close to vanishing cold electron density in the center of the AKR source.

The energetic electrons (Plate 1b) form a widely spread downgoing beam of energy between 5 and 20 keV. At the same time, close to 10 keV energy upgoing ion beams appear in Plate 1a in the center of the AKR source.

At the locations where the spacecraft enters the AKR source, crossing its equatorial border at 0616:32 UT, and where it leaves the source, crossing the polar border of the source at 0616:57 UT, strong perpendicular electron heating up to keV energies is observed in the electron distribution with peak flux at 90° and 270° as has been reported by *Pottelette et al.* [1999]. The drop in ion energy observed simultaneously indicates that the spacecraft crossed the narrow region where the ionospheric ion background is accelerated upward until it forms the ion beam encountered in the AKR source.

The nature of the broadband wave noise in the AKR source boundaries has been discussed by *Pottelette et al.* [1999]. This noise appears in coincidence with the perpendicularly heated electrons. It has been shown to be entirely electrostatic and consisting of coherent, narrow, spatially well separated wave packets [cf. *Pottelette et al.* [1999], Figure 2]. The electric field of the broadband noise is polarized mainly parallel to the ambient magnetic field. It has been argued there that most of this spectrum propagates in the electron acoustic mode which is generated in presence of a mixture of hot and cold electrons when the cold electron

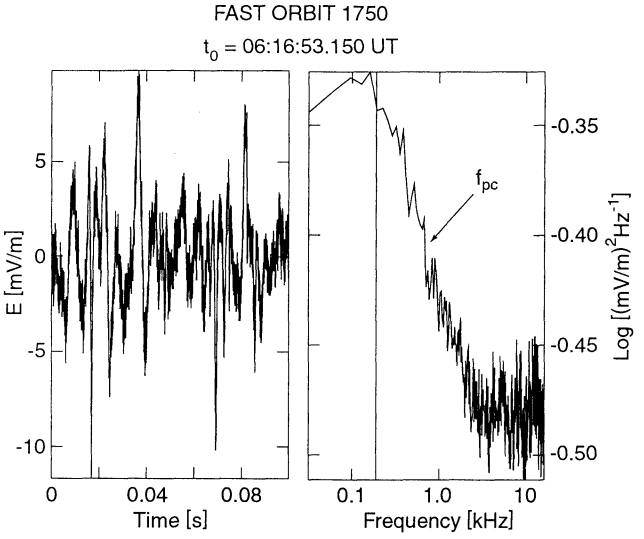

Figure 1. (left) Wave form and (right) Spectrum of the low frequency broadband emission in the acceleration region indicating the presence of electron acoustic waves. From the upper frequency cutoff of this noise at ~800 Hz one obtains an estimate of the residual cold electron plasma density $n_c/n_h \approx 3\%$.

density is higher than in the AKR source region itself. This is in agreement with the incomplete acceleration of ions and electrons in this region. The spectrum of this emission also contains a component in the ion acoustic mode.

Figure 2 displays the variation of the moments calculated from electron spectrometer data. These calculation neglect particle fluxes below 80 eV in order to avoid the contribution of photoelectrons. Note that in the narrow transition region the parallel electron temperature drops from several keV to a few 100 eV.

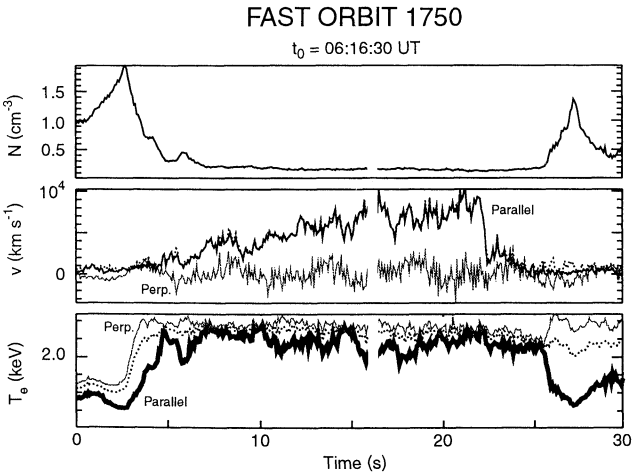

Figure 2. Electron moments during crossing of the upward current region. Note the steep 1 order of magnitude drop in parallel electron temperature (bottom panel) at second 26 when the spacecraft crosses the acceleration region. Here the cold electron density becomes substantial.

2.2. Narrowband Drifting Radiation Sources

The event in which we are interested took place during the period when FAST was in the center of the AKR source region at time 0616:48 UT. It occupies only 6 s of time. The event was observed by the wave tracker instrumentation aboard FAST [*Ergun et al.*, 1998b]. The bandwidth of each tracker snapshot is 16 kHz with 100-Hz resolution, and the time resolution per sweep is 16 ms. The duration of the tracking time in each window was fixed to 1 s. The wave tracker tries to detect the maximum intensity of the emission. When it has found an emission maximum it tries to follow its motion across the spectrum.

The event that attracts our interest appears in Plate 1e as the intense drifting emission starting near ~368 kHz and moving up to ~390 kHz within ~5 s. The bandwidth of this emission is of the order of only 1 kHz. Since the local cyclotron frequency during this time interval was near ~340 kHz, this drifting emission feature is well above the resonant maser emission frequency which by maser theory in the relativistic case should maximize even below the electron-cyclotron frequency. This implies that we observe a strongly localized drifting AKR source situated roughly ~140 km below spacecraft. The increase in emission frequency indicates that the structure is moving along the magnetic field downward into the ionosphere. Somewhat closer inspection of the emission also shows that it is highly variable in bandwidth and intensity while its spectral drift is practically constant moving at a rate of $\sim +4.5\,\mathrm{kHz\,s^{-1}}$ which corresponds to a downward displacement velocity of $v_{\|} \approx 45\,\mathrm{km\,s^{-1}}$.

Plate 1f shows another example of narrow band drifting structures well above the local cyclotron frequency observed in FAST orbit 1761 (on January 31, 1997) at 0644:56 UT. The overall event was described by *Strangeway et al.* [1998] in their Figure 1. As in orbit 1750, the spacecraft on this orbit was also inside the AKR source. The high frequency suggests a generation altitude below spacecraft. In contrast to orbit 1750 the tracker simultaneously detected two narrow band emission features at different central frequencies. The two features are highly variable in bandwidth and emissivity. It is obvious from Plate 1f that they behave about independently. The higher-frequency feature is nearly stationary while the lower frequency feature moves upward in the spectrum. At the end of the event the two features approach each other and start moving in company, apparently staying for a while in constant separation distance of ~3 kHz, which corresponds to roughly 15 km along **B**. Interestingly, the two radiation sources do not merge. Instead, the lower-frequency source approaching the higher-frequency source from above pushes the latter down the field line. This is the first observation of this kind. We interpret it as the interaction of two electric field layers of equal polarity which we identify below tentatively as ion holes.

2.3. Fine Structure of Drifting Events

The drifting features seen in Plates 1e and 1f exhibit a number of interesting properties. First, the main feature is extraordinarily narrowband. The instantaneous bandwidth being of the order of not more than 1 kHz. Second, the feature drifts at nearly constant speed of $+(4-5)\,\mathrm{kHz\,s^{-1}}$. Third, closer inspection of the dynamic spectrum uncovers some even more interesting properties. The weak emissions both above and below the main drifting emission exhibit themselves a frequency drift which is much faster than that of the main slowly drifting feature. Fast drifts like these correspond to small-scale localized radiation sources which move at velocities in the range of 300-1000 $\mathrm{km\,s^{-1}}$ along the field. The average value of the drift speed of these sources is ~500 $\mathrm{km\,s^{-1}}$. Both types of elementary localized radiators, above and below the latter, seem in the average to drift toward the main structure in a way as if they are attracted by it. During this motion they amplify and when dropping into the main structure they seem to make up a large part of the emission from the main feature.

The tracker recordings of the drifting structures during FAST orbit 1761 (Plate 1f) show a similar but slightly different behavior. Here the main structures were nearly immobile but split into two different events one drifting the other not drifting. Figure 3 shows a high-time resolution plot of the most interesting part of this event. Inspection of the drifting and nondrifting features reveals that the emission is practically made up of the narrow but fast drifting features which seem to be captured inside the main feature and sometimes even turn around. This is particularly well seen in the upper part of the emission at second 1-2 where one clearly observes fine-scale features to turn around at the very center of the slowly drifting or even standing main emission. In this case the fast drifting features come from both sides and stop in the center. In other cases one also observes that a structure continues across the main feature. We will go into more detail when describing an interpretation of these events in a heuristic model of AKR fine structures we are going to develop below. Another example of a narrow band feature detected on orbit 1773 is shown in Figure 4. Here the main feature is nearly stationary over most of the observational tracker period. As in the other cases, however, closer inspection shows that this main feature as well consists of a large number of narrow band fast drifting emission events which accumulate in its center. Apparently, they are attracted from both sides to the center in this case.

3. Discussion

3.1. General Considerations

The current observation of the AKR fine structure in the AKR source region must be viewed in the light of the general characteristics of the AKR source as presented by *Ergun et al.* [1998a] and *Strangeway et al.* [1998, 2000]. Their conclusions may be summarized as follows: the AKR source region coincides largely with the auroral low-density acceleration region. Since this region carries an upgoing field-aligned current, one observes in addition to the precipitating hot auroral electrons upgoing ion and downgoing electron beams.

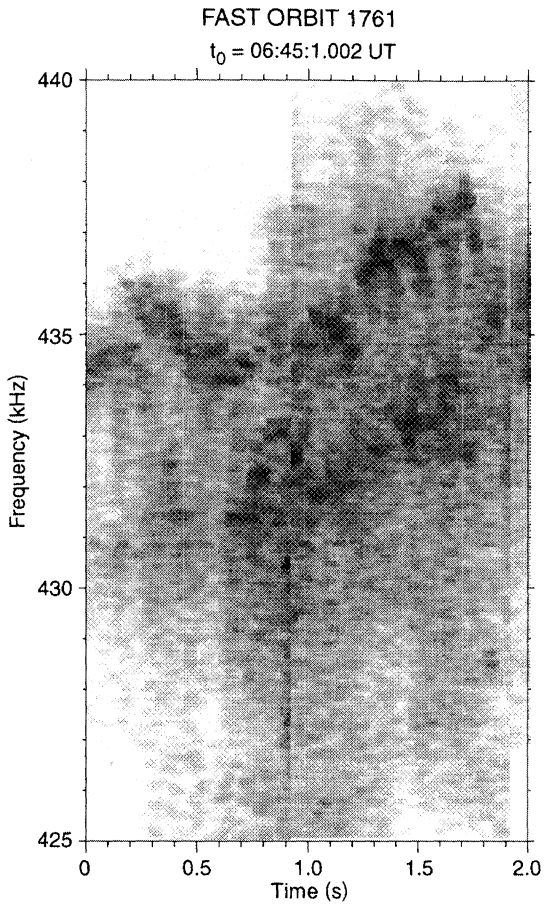

Figure 3. High time and frequency resolution plot of tracker data for the orbit 1761 event in Plate 1f. Elementary radiation sources moving downward (upward in frequency) are reflected at the position of the main emission band. At their turning points they cause the strongest intensity in AKR. When moving upward (to lower frequencies) the emission weakens again. Many of these structures overlay to compose an apparently continuous AKR emission.

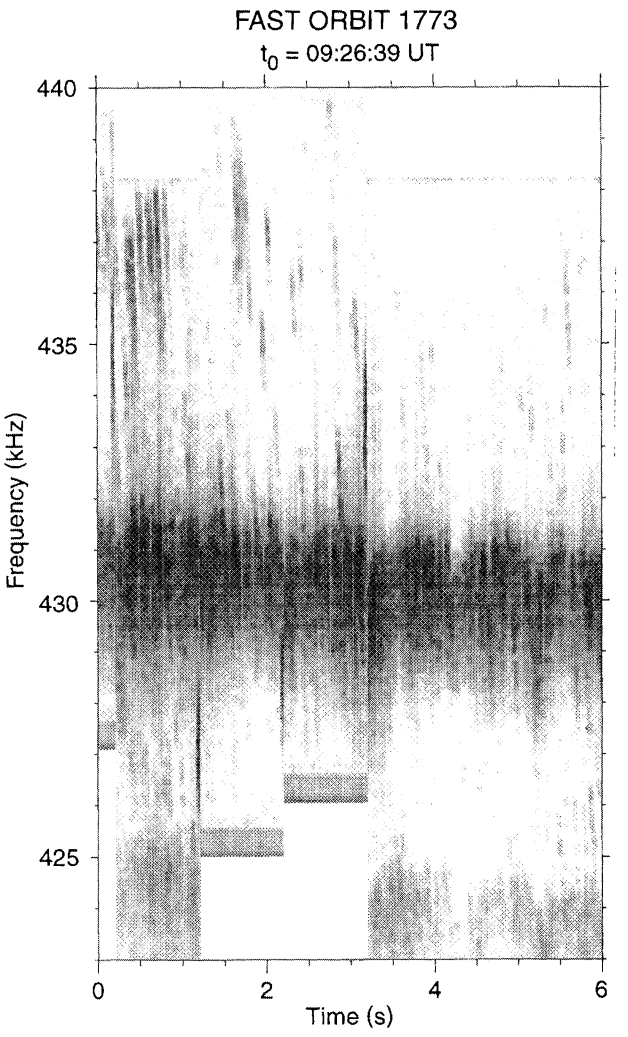

Figure 4. Wave tracker recording during FAST orbit 1773. The plot shows a nearly stationary ($v_{||} \approx 0$) narrow band emission feature at $\sim$430 kHz. The band is obviously composed of many small emission events. Most of these perform high-frequency drifts toward and away from the band identifying the band as an reflector for the elementary emitters.

Contrary to previous model assumptions where the electrons have been assumed to possess a loss cone distribution, the hot auroral electrons form a particular distribution which consists of a field-aligned part and an incomplete ring distribution with almost no electrons in the reflected cone. Strong evidence for the presence of such distributions, which have been given the name of horseshoe distributions, has been provided by FAST [*Delory et al.*, 1998]. The ring-like part is produced by mirroring of auroral electrons under the action of the mirror force in the magnetic field and by additional downward acceleration in the same field-aligned electric potential that accelerates the ion beam upwardly. The presence of this field-aligned potential drop also ensures that the residual amount of cold electrons is small.

Under these conditions the electron-cyclotron maser has been shown to not being fed by the loss cone but taking its free energy from the horseshoe distribution and thus effectively from the field-aligned electric potential [*Ergun et al.*, 1998a; *Pritchett et al.*, 1999]. It is crucial that the emitted radiation has its maximum below the local nonrelativistic electron-cyclotron frequency f_{ce} close to the relativistic R-X-mode cutoff $f_{\mathrm{RX}u,r} < f_{ce}$, which for weakly relativistic electrons even is also below the local electron-cyclotron frequency. This has first been demonstrated by *Pritchett* [1984] and *Strangeway* [1985] and agrees perfectly with observation. It provides a strong argument for the presence of the horseshoe maser action in generation of AKR.

To make clear what is meant here, we note that the free-space electromagnetic R-X mode in plasma in magnetoionic theory has a low-frequency cutoff $f_{\mathrm{RX}u} \simeq f_{ce} + f_{pe}^2/f_{ce}$ at wavenumber $k = 0$ above the (nonrelativistic) cyclotron frequency where the wave is reflected. Taking into account

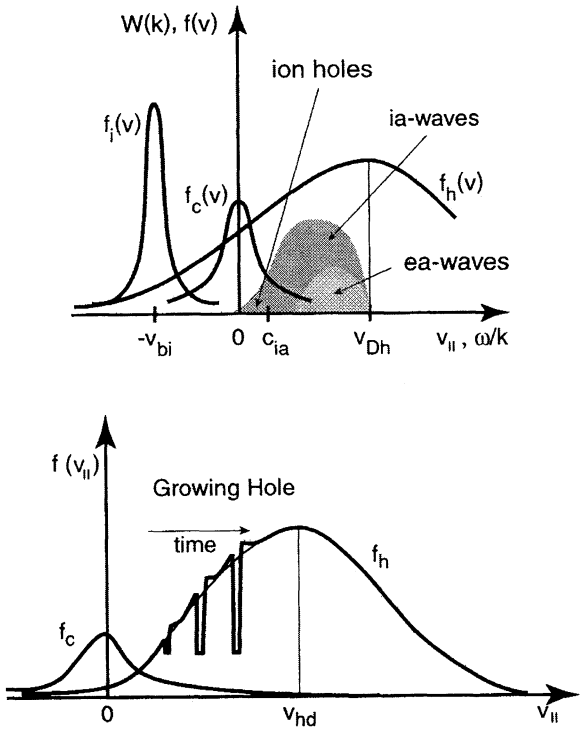

Figure 5. (top) Sketch of the particle distribution functions $f(v)$. Unstable spectra $W(k)$ of electron and ion acoustic waves as function of wave phase speed ω/k are indicated by shading. Both types of waves move downward in the cold electron and ion frames. (bottom) The mechanism of electron hole growth when a hole is moving into the hot particle distribution $f_h(v_{||})$.

the relativistic effect, the cyclotron frequency is replaced by f_{ce}/γ where $\gamma = (1 - v^2/c^2)^{-1/2}$, which reduces the cyclotron frequency as well as the cut-off. At the same time the maser resonance condition $k_{||}v_{||} = 2\pi[f - f_{ce}/\gamma(v_{||}, v_\perp)]$ shows that the relativistic resonance line in $(v_\perp, v_{||})$-space becomes a circle for $k_{||} = 0$ and therefore lies entirely inside the horseshoe distribution. Thus the horseshoe distribution favors strictly perpendicular propagation of the X mode for largest growth rate.

The properties of the electron-cyclotron maser radiation generated by the horseshoe have been discussed in the above references (see also *Ergun et al.* [2000]). The group velocity of the excited mode is about perpendicular to the local magnetic field at excitation site which lies in the general auroral density cavity ($f_{pe} \ll f_{ce}$). Propagating away from the excitation site, spatial and temporal variations of the local plasma density cause corresponding variations in the R-X mode cutoff and lead to scattering of the radiation during propagation away from the place where it has been generated. The picture is complicated by the dependence of the cutoff from resonant particle energy. The relativistic effect for too low-energy particles is too weak to reduce the cutoff sufficiently for escape of the radiation. On the other hand, since the cyclotron and plasma frequencies both increase toward the downward direction, most of the radiation energy will be ultimately reflected upward and, unless reabsorbed at a site where its frequency matches the local upper hybrid resonance, it will be directed by scattering away from Earth. This discussion thus lets us expect that the radiation is channeled away from Earth into free space where it can be observed by spacecraft like FAST.

Adopting this point of view, we may immediately conclude that the high-frequency drifting AKR structures we present in this note cannot have been generated locally at the position of the spacecraft. They are at a much too high frequency, well above the local electron-cyclotron frequency, and in addition exhibit a frequency drift which cannot be brought into accord with any changes in the local f_{ce}. It is natural to assume that the emission has been generated at a remote location relatively far below the FAST spacecraft in

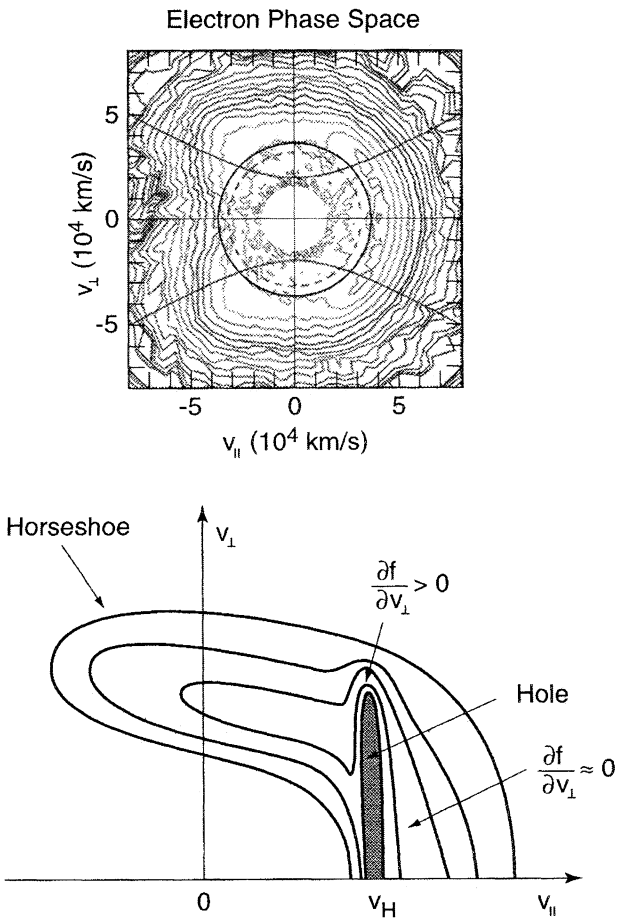

Figure 6. (top) Sketch of the horseshoe distribution as measured by FAST [after *Delory et al.*, 1998]. The hyperbolas are the lines which mark the borders between trapped and lifted particles in a field-aligned electric potential field. The inner part of the distribution has been cut out because it is populated by photo electrons. (bottom) Schematic of the local deformation of the distribution by an electron hole moving at speed $v_H < v_{h,th}$ downward. The isodensity lines are deformed by the presence of the hole.

a much stronger field region. The emitter of the radiation has obviously been moving along the field in order to account for the rapid frequency drift of the radiation feature. In addition, the source must have been highly localized in space. This is suggested by the overall narrow bandwidth of the emission of $\Delta f \sim 1$ kHz. This bandwidth corresponds to a distance of $\Delta s \sim 5$ km along the magnetic field.

Even more intriguing than this general argument is the existence of the very large number of extraordinarily fast drifting emission features. Their instantaneous bandwidths sometimes amount to the order of only ~100 Hz and occasionally may have been even less and unresolvable by the instrument. Note that such narrow bandwidths have been suspected already earlier but have not been taken for serious in the literature [e.g., *Strangeway et al.*, 2000]. The elementary features might have field-aligned extensions from a few 100 m to 1 km only while their perpendicular scale may be down to the several 10-m range. In many cases they seem to be attracted by the main slower drifting source both from below and from above.

Figure 3 shows an example of this attraction with the fast drifting elementary emission sources approaching the main feature from above (increasing frequency), being reflected when hitting the main feature and returning upward along the magnetic field. Many of these elementary features radiate strongest during the short time interval of their reflection. Closer inspection of Figure 3 even suggests that except for the main features, almost all of the radiation in Figure 3 is made up of elementary emission events. AKR seems to consist of the accumulate effect of very many such tiny point sources contributing to the broad spectrum. The fainter elementary radiation features in Figure 3 emit the radiation under an unfavorable angle for detection by the spacecraft. This can be understood when referring to the high degree of directivity of the emission of radiation. In the horseshoe electron-cyclotron maser mechanism, radiation is emitted nearly perpendicularly (within ~2° of the normal to the local magnetic field direction) propagating in the X mode.

The most tantalizing among the problems posed by the above observation of the large number of elementary drifting AKR sources raises the following questions: (1) Why is the radiation produced in such narrow elementary features? (2) What is the nature of the fast and slow drifting features? (3) What causes the reflection of the elementary radiators? In other words: Why seem the elementary features to be attracted by the main and slowly drifting source? (4) Why is the emission at the reflection point in many cases the most intense?

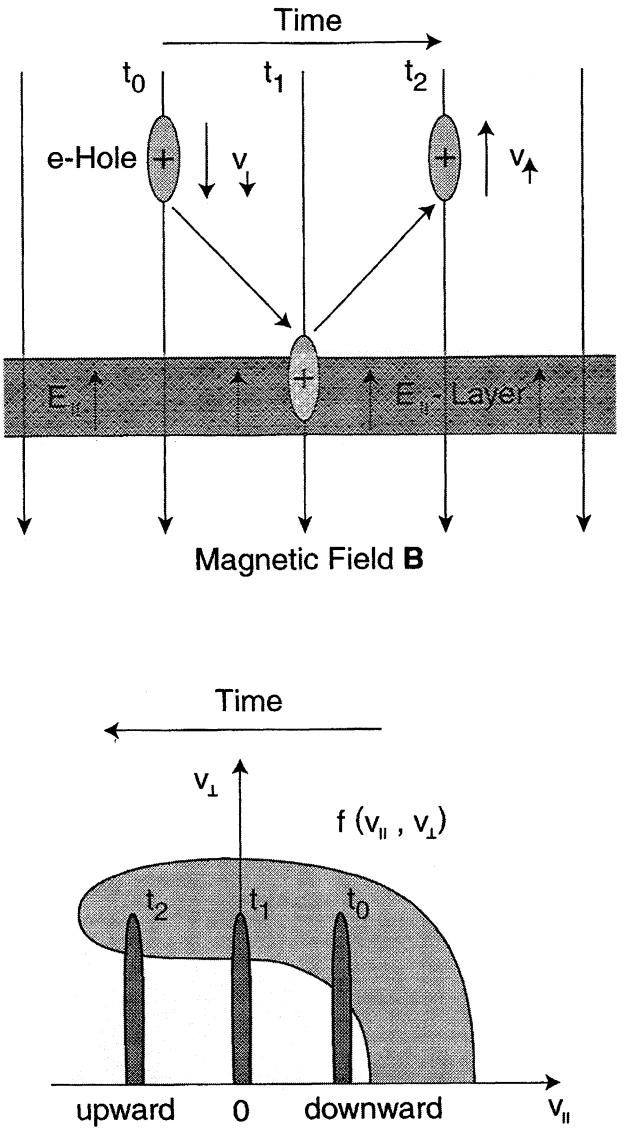

Figure 7. (top) Reflection of a hole at the $E_{||}$ layer when the hole coming from above and being a positive charge is rejected by the field-aligned electric field. (bottom) The resulting deceleration of the hole in phase space. The hole moves toward $v = 0$ parallel velocity and at negative (upward) speeds leaves the horseshoe distribution. Under these conditions it ceases generating radiation.

3.2. Electron Hole Dynamics

It is not easy to answer these questions definitively. Here we attempt a more speculative explanation.

There are only few possibilities which can lead to narrowband emissions when sticking to the horseshoe electron-cyclotron maser, in particular when considering fast plasma drifts along the magnetic field. *Pritchett et al.* [1999] have provided arguments based on numerical simulations of AKR horseshoe maser emission in the auroral density cavity that the bandwidth can hardly be less than ~1 kHz. The bandwidths reported in the present paper are smaller by roughly 1 order of magnitude and can therefore hardly be explained by spatial amplification effects in the above model. Moreover, the whole picture of high spectral resolution AKR emission strongly suggests that a large part of the emission itself is made up of narrowband fast drifting structures which we believe to be real elementary emitters. The simplest assumption is thus still to identify the emission sources with such real, drifting small-scale physical objects.

In order of being able to emit, these objects must be em-

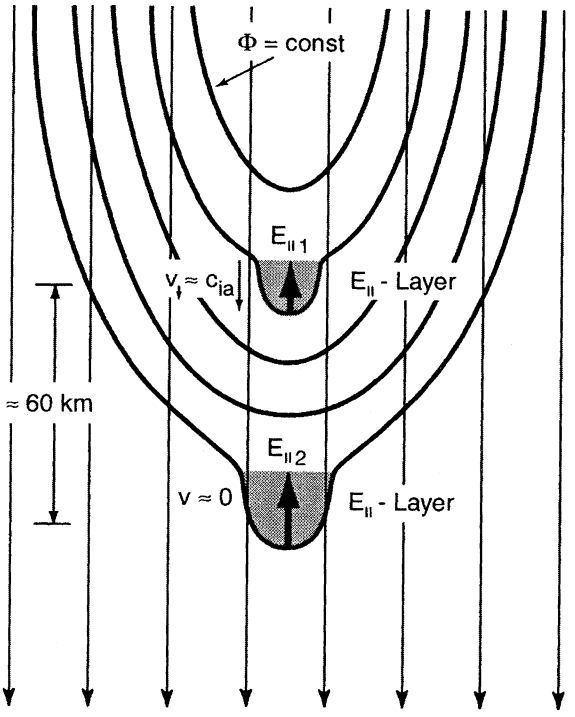

Figure 8. Schematic of the interaction of two $E_{||}$ layers of same polarity and initial field-aligned separation of ~60 km as suggested by the observations. The upper layer ($E_{||1}$) moves down (increasing gyrofrequency f_{ce}) at about ion acoustic velocity ($v_{||} \sim c_{ia}$) toward the stationary (velocity $v_{||}$ ~0) lower lying layer ($E_{||2}$). When interacting with $E_{||2}$, it either will come to rest or push the lower layer downward at about same speed (see Plate 1f). The electric equipotentials are assumed to be small- or mesoscale with transverse dimension the order of some ~10 km as suggested by the observation. Many such layers may make up a large-scale potential of some approximately kV (as suggested by *Ergun et al.* [1998a]), capable of accelerating ions to keV energies. Nothing is said here about the physical nature of such electric field layers, but under the conditions in the auroral magnetosphere as investigated in the present paper, it seems reasonable to assume that such layers are connected with ion acoustic structures [*Gray et al.*, 1991] which show all properties of ion holes.

bedded into an unstable particle distribution and must be able to stimulate radiation. Though there is some similarity in the emission feature with interplanetary type III or *U* bursts, the emission cannot have been caused by drifting electron bunches emitting close to the plasma frequency or its harmonics. This is inhibited by two facts: the smallness of the plasma frequency in the auroral source which would require that the observed emission is an extremely high harmonic of the plasma frequency which in itself is an entirely impossible assumption. The other fact is the comparably slow drift speed of the elementary sources which is far below any acceptable electron beam speed and would restrict the resonant excitation to the zero-energy electrons. Such electrons are far away from any resonance and can cause nothing but Landau damping. Thus the sources must be related to nonlinear wave features that evolve in the auroral AKR source.

When transforming the frequency drifts into spatial velocities, the slowly moving main features propagate at a velocity ranging from some 10-100 km s^{-1}, obviously sometimes with high variability (cf. for instance the difference in the drifts of the main structures in Plates 1e and 1f). As the data of orbit 1761 (Plate 1f) show, the speed of one single event may even change drastically especially when two such features undergo mutual interaction. The range of the observed velocities does not allow to identify the structures with one particular known single wave mode of a hot plasma as a causative agent though it roughly matches that of ion acoustic waves. This suggests that these slowly drifting structures are nonlinear features evolving under the local conditions met in the auroral plasma.

The most probable such features are ion holes which are formed during the nonlinear evolution of ion acoustic waves as is known from numerical simulations [*Gray et al.*, 1991]. These simulations also showed that interacting holes experience strong variations in their drift velocities. They even may reverse their direction while remaining their integrity. This is possible when the velocity change happens on a faster timescale than the decay time of the hole. Note also that the velocity is not galilean invariant such that the observed velocity may not coincide with the speed of the structure relative to the background plasma. It is the latter that determines the range of existence of the holes.

The fast moving elementary features, on the other hand, have speeds which are generally larger than several 100 km s^{-1} when they are sufficiently far away from their location of reflection. Speeds of this magnitude fall into the range of electron acoustic velocities, depending on the temperature of hot electrons and the cold-to-hot electron density ratio. Transforming the instantaneous bandwidth of these elementary events into a longitudinal spatial extension the size of the elementary events will be of the order of $\sim 3 - 10\,\lambda_D$ which is roughly comparable to the expected sizes of nonlinear electron acoustic waves which under certain conditions may evolve into electron solitary structures [*Dubouloz et al.*, 1991, 1993] or electron holes [*Omura et al.*, 1996; *Berthomier*, 2000].

Electron hole formation in presence of a ring or horseshoe distribution has not yet been explored theoretically and is outside of this paper. However, in analogy to the known evolution of electron holes we propose a qualitative model which partially explains a number of properties of the elementary radiation events. Electron holes evolve in the interaction of hot and cold electron plasma [*Omura et al.*, 1996]. They are known as nonlinear BGK modes [*Muschietti et al.*, 1999]. Such nonlinear states are similar to ion holes which evolve in the nonlinear state of the ion acoustic instability [e.g., *Gray et al.*, 1991; *Berthomier et al.*, 1998] which is driven by the difference in electron and ion drifts. In analogy, in the electron hole case the source of free energy is

the difference in the drifts and temperatures of the hot and cold electron populations [*Omura et al.*, 1996; *Berthomier*, 2000]. In this view the hot-cold electron plasma interaction excites electron acoustic waves which evolve into solitary waves which in certain parameter ranges form electron holes.

Figure 5 shows the schematic evolution of such a one-dimensional hole for a given hot-cold electron distribution configuration. Since the density of the electron hole is conserved, it effectively grows when moving into the denser part of the electron distribution. When the hot plasma dominates this is the hot distribution. Since the hole is a localized decrease in electron number [*Muschietti et al.*, 1999] it implies a decrease in electron density and, at the same time, an increase in velocity space gradient in the region of the hole. Depending on the direction of this gradient it might be in favor or not of generation of radiation. (Note that increases in density as expected for compression act in a similar way but are not in favor of radiation because they violate the condition of most intense emission [*Strangeway*, 1986], which is coupled to the relativistic drop of the X-mode cutoff below f_{ce}.) In addition, the hole contains a dilute heated plasma component, slightly hotter than the environment. In phase space this appears as small bulges at the boundaries of the hole.

There may exist different types of electron holes. The ones that resemble most simple finite though small amplitude solitons of the kind of Korteweg-deVries (KdV) solutions obey an inverse proportionality between their size and their amplitudes and speeds. Another class whose shape deviates considerably from the KdV bell-shaped solitons, has larger amplitude. In certain parameter regimes its amplitudes increase with size and speed. This property was recovered by *Muschietti et al.* [1999] from a BGK solution in a two component electron plasma.

Berthomier [2000] has investigated electron acoustic solitary waves within the full parameter space and has shown that these solutions evolve in the nonlinear state of such plasmas even in the fluid approximation. They can thus be understood as another family of solitary solutions. KdV solitons occupy only a subvolume of the parameter space which is of very small measure. Thus the more general electron acoustic solitary structures correspond closely to electron holes and obey the same dependence on size and speed attributed to those. The propagation speed of a hole is related to the electron acoustic solitary wave speed which spans a wide range but is generally slower than the hot electron thermal speed. When considering an additional drift of the hot component, the holes are riding on the drifting part of the distribution. One thus expects that the holes, which we believe form the elementary radiation sources, propagate downward in the upward current region together with the hot electron component but at a lesser velocity.

Though the dynamics of electron holes is different from that of ion holes, one can qualitatively stress the formal analogy to ion holes and suggest that the drift velocity of an electron hole should not necessarily be conserved but will change when the hole interacts with either other electron holes or when it occasionally encounters an ion hole. This is just what is observed in the data.

Each electron hole, being a depletion in electron density, cuts out a certain interval of the electron phase space. This is shown schematically in Figure 6 where the hole appears as a narrow strip in phase space. Clearly, electrons with high parallel speeds having much larger energy than the hole potential in the moving frame of the hole are not affected. On the other hand, the range of perpendicular velocities involved is large, typically of the order of the hot thermal speed of the electrons as indicated in Figure 6. Observations of the POLAR spacecraft indicate that electron holes are rather spherically symmetric [*Franz et al.*, 2000], a conclusion which has also been drawn by *Berthomier* [2000] from simplified magnetized theory in strong magnetic fields. Because electron holes possess a lack of negative charges, they are positively charged entities possessing a positive potential. The Debye length amounts to a few 100 m. Typical spatial sizes thus range from 100 m to few kilometers.

3.3. Modulation of Radiation by Electron Holes

In order to provide a heuristic argument for the modulation of the radiation in presence of an electron hole let us inspect Figure 6, which suggests that the hole has two effects on the distribution. The part overlapping the horseshoe distribution decreases the density and introduces additional phase space gradients. In the theory of the electron-cyclotron maser emission the gradient relevant for generation of radiation is the partial perpendicular velocity gradient on the electron distribution function $f(v_{\|}, v_{\perp})$, namely, $\partial f(v_{\perp}, v_{\|}, t)/\partial v_{\perp}$, where $v_{\perp}$ is the component of the velocity perpendicular to the magnetic field. Since the horseshoe distribution corresponds to an incomplete electron ring in phase space the derivative of the distribution function with respect to $v_{\perp}$ can be expressed as the sum of two terms, the first one is the derivative with respect to electron pitch angle α, the second is the derivative with respect to electron velocity v:

$$\frac{\partial f}{\partial v_{\perp}} = \frac{\cos\alpha}{v}\frac{\partial f}{\partial \alpha} + \sin\alpha\frac{\partial f}{\partial v}$$

Because of the symmetry of the distribution function, the derivative $\partial/\partial\alpha \approx 0$ with respect to α can be neglected in the right half plane, yielding $\partial f/\partial v_{\perp} \approx \sin\alpha\,\partial f/\partial v$. Clearly, for $\alpha \approx 0$ this expression vanishes and is maximum somewhere close to $\alpha \sim \pi/2$. Hence, an electron hole generated close to the center of the horseshoe and decelerated to zero velocity will encounter increasingly favorable conditions for local generation of radiation. Moreover, its finite extension in $v_{\|}$ and $v_{\perp}$ causes additional local perpendicular gradients on the distribution as indicated by the isodensity lines in Figure 6. These do also favor emission or radiation when contributing to the perpendicular phase space gradient in the relativistic emission process. Qualitatively, we may thus expect that an electron hole self-consistently evolving in the horseshoe distribution can produce elementary radiation of the kind observed with highest emissivity when the

hole is retarded and comes about to rest. In particular, at its reflection point the hole will radiate strongest because of the coincidence of the above conditions, $\sin\alpha \sim 1$ and the steep gradient in v. This will add to the total emission from the entire horseshoe and cause its fine structure.

Retardation of the electron hole can be caused when the electron hole riding on the back of the hot electron population during its downward motion enters the region of the upward directed electric field which accelerates ions upward and electrons downward. Since the electron hole effectively is a small mass (and hence small momentum) positive charge in the electron plasma it will be retarded by the upward electric field and will be reflected until ultimately becoming accelerated upward again. This is precisely the case seen in the observations. Figure 7 visualizes such a model. Thus, in the presence of a reflecting parallel electric potential drop electron holes may even come briefly to rest with respect to the plasma. This is different from electron holes moving in an electrically neutral plasma where their speed relative to the plasma background is prevented from becoming zero.

We can estimate the power emitted in one elementary radiation event. The color code respectively gray scale in the measurements (not shown in Plates 1e, and 1f and Figures 3 and 4) indicate an electric field intensity of $\langle E^2\rangle \approx 10^{-5} - 10^{-6}\,(\Delta f/\mathrm{Hz})\ \mathrm{V^2m^{-2}}$ for each of the intense elementary radiation sources. The bandwidth of the elementary radiation source is about $\Delta f \approx 100$ Hz. Assuming a distance between source and satellite of roughly $D \approx 100\,\mathrm{km}$, the above intensity corresponds to an AKR power of

$$P(f) \approx 10^{3-4}\left(\frac{\Delta f}{100\,\mathrm{Hz}}\right)\left(\frac{D}{10^5\,\mathrm{m}}\right)^2\left(\frac{\Delta\Omega}{\pi}\right)\ \mathrm{W}$$

typically emitted by each of the elementary events. Here Δf and D are measured in the units as indicated, and we assumed that the radiation is emitted into a solid angle $\Delta\Omega = \pi$ where we take into account that the radiation is partially directed when escaping from the source to free space. When the directivity of radiation is more pronounced, the estimated power is reduced.

The above estimate gives is a relatively large power emitted per elementary radiation source. The observation (cf. Figures 3 and 4) suggests that there are many of such elementary sources in one AKR event which contribute to the total emission in AKR. In order to reproduce the total instantaneous power of $P_{\mathrm{tot}} \approx 10^{7-9}\,\mathrm{W}$ in AKR, one thus needs between 10^{4-6} such elementary radiators. Each of them should have a typical volume of $10^9\,\mathrm{m^3}$. If all radiators are densely packed into a cube this yields a total volume of $V \approx 10^{13-15}\,\mathrm{m^3}$ or a side length $L \sim 20 - 100\,\mathrm{km}$ of the cube for the entire AKR source. Such a total volume is in reasonable agreement with the expected size of the radiation source in total. We therefore conclude that a substantial part of the AKR emission seems to be made up of spatially localized small moving emitters which interact with the general horseshoe distribution and are themselves generated by nonlinear interaction in the hot electron plasma in the auroral zone.

4. Conclusions

In summary, we have shown that the AKR under "normal" conditions is composed of a large number of elementary radiation events, which either make up for all the radiation or may be superposed on a continuum radiation background. They move at moderate speeds along the magnetic field, which are in the range of the electron and ion acoustic velocities. These elementary radiation events have their sources in spatially localized wave structures which are located at the edges of the auroral upward current density cavity.

We have intentionally identified the faster drifting entities as electron holes/electron acoustic solitary structures of relatively small size. These features are excited by the temperature difference between the dilute cool electron background still present in the edge region and the hot approximately few keV electric field accelerated electron plasma drifting downward in the upward electric field region. The elementary radiation sources ride on the hot component but at a considerably lower speed. Being electron holes they appear as positive charges on the electron horseshoe background distribution, deforming this distribution and contributing to favored weakly relativistic radio emission. Moving downward along the magnetic field line the elementary radiation sources are retarded and reflected from the general field-aligned upward electric field which is present in the electric field layer. When reaching zero speed, radio emission is most amplified by the holes. After reflection the holes move upward again and cause only weak emission. The radiation emitted by the elementary sources will be scattered at density inhomogeneities and will ultimately escape from the cavity and reach the spacecraft.

Observation of fine structure of this kind provides information about the local dynamics of the auroral zone turbulence. In particular it provides an indication of the existence of layers carrying parallel electric potential drops as shown schematically in Figure 8. It moreover suggests that at a particular time there may exist several highly localized such field-aligned electric field layers of field-aligned extension of merely a few km in the auroral acceleration region. This gives very strong support to the idea that most of the large-scale auroral field-aligned potential drop is made up of many mesoscale structures adding up to the $\sim$10 keV large-scale electric potential drop as proposed by *Boström et al.* [1988], *Pottelette et al.* [1993], *Carlson et al.* [1998b], and *Ergun et al.* [1998a].

We have presented the first remote observation of such localized potential layers and their mutual interaction. This was possible only on the way of analyzing the fine structure of remotely detected AKR. These layers, in our observations found in the upward current region, are of same generally upward polarity, as can be inferred from their repulsive interaction which is obvious from Plate 1f.

The large number of elementary sources, which are seen in the high resolution measurements (Figures 3 and 4) of AKR, also suggests that a substantial fraction of AKR is generated in such elementary sources. This again provides further support for the newly developed model [*Pritchett and*

Strangeway, 1985; *Strangeway et al.*, 1998; *Ergun et al.*, 1998a, 1998b; *Pritchett et al.*, 1999] of relativistic horseshoe-maser generated radio emission in very dilute low-β plasma while suggesting its modification in order to include the existence of the large number of elementary radiators reported in the present paper.

Acknowledgments. The FAST mission is a project of the Space Sciences Laboratory of the University of California at Berkeley run under the auspices of NASA. The authors are indebted to C. W. Carlson and R. E. Ergun for providing the particle and wave data as well as for some useful discussions. They also thank P. L. Pritchett, R. J. Strangeway and R. R. Anderson for comments and discussions. Thanks are due to the referees for their constructive suggestions. In addition, R.A.T. thanks the directors of ISSI, Johannes Geiss, Götz Paschmann, and Rudolf von Steiger as well as the ISSI staff for their hospitality during his long-term visit at ISSI, Bern, where most of this work has been performed. This research is part of the France-Berkeley Program. Part of the work was supported by the PROCOPE cooperation under contract numbers D/9822921 and 99057.

Janet G. Luhmann thanks Philip Pritchett and Paul M. Kintner for their assistance in evaluating this paper.

References

Berthomier, M., Turbulence et Accélération dans les Zones Aurorales Terrestres, Ph.D. thesis, 164 pp., University of Paris VI, January 2000.

Berthomier, M., R. Pottelette, and M. Malingre, Solitary waves and weak double layers in a two electron temperature auroral plasma, *J. Geophys. Res.*, *103*, 4261-4268, 1998.

Berthomier, M., R. Pottelette, and R. A. Treumann, Parametric study of kinetic Alfvén solitons in a two electron temperature plasma, *Phys. Plasmas*, *16*, 467-475, 1999.

Boström, R., G. Gustafsson, B. Holback, G. Holmgren, H. Koskinen, and P. Kintner, Characteristics of solitary waves and weak double layers in the magnetospheric plasma, *Phys. Rev. Lett.*, *61*, 82-85, 1988.

Carlson, C. W., R. F. Pfaff, and J. G. Watzin, The Fast Auroral SnapshoT (FAST) mission, *Geophys. Res. Lett.*, *25*, 2013-2016, 1998a.

Carlson, C. W., et al., FAST observations in the downward auroral current region: Energetic upgoing electron beams, parallel potential drops, and ion heating, *Geophys. Res. Lett.*, *25*, 2017-2020, 1998b.

Chiu, Y. T., and M. Schulz, Self-consistent particle and parallel electrostatic field distributions in the magnetospheric-ionospheric auroral region, *J. Geophys. Res.*, *83*, 629-638, 1978.

Delory, G. T., R. E. Ergun, C. W. Carlson, L. Muschietti, C. C. Chaston, W. Peria, J. P. McFadden, and R. Strangeway, FAST observations of electron distributions within AKR source regions, *Geophys. Res. Lett.*, *25*, 2069-2072, 1998.

Dubouloz, N., R. Pottelette, M. Malingre, and R. A. Treumann, Generation of broadband noise by electron acoustic solitons, *Geophys. Res. Lett.*, *18*, 155-158, 1991.

Dubouloz, N., R. A. Treumann, and R. Pottelette, Turbulence generated by a gas of electron-acoustic solitons, *J. Geophys. Res.*, *98*, 17415-17422, 1993.

Ergun, R. E., et al., FAST satellite observations of large amplitude solitary structures, *Geophys. Res. Lett.*, *25*, 2041-2044, 1998a.

Ergun, R. E., et al., FAST satellite wave observations in the AKR source region, *Geophys. Res. Lett.*, *25*, 2061-2064, 1998b.

Ergun, R. E., C. W. Carlson, L. Muschietti, I. Roth, and J. P. McFadden, Properties of fast solitary structures, *Nonlin. Proc. Geophys.*, *6*, 187-194, 1999.

Ergun, R. E., C. W. Carlson, J. P. McFadden, G. T. Delory, R. J. Strangeway, and P. L. Pritchett, Electron-cyclotron maser driven by charged-particle acceleration from quasi-static magnetic field-aligned potentials, *Astrophys. J.*, in press, 2000.

Franz, J. R., P. M. Kintner, C. E. Seyler, J. S. Pickett, and J. D. Scudder, On the perpendicular scale of electron phase-space holes, *Geophys. Res. Lett.*, *27*, 169-172, 2000.

Gray, P. C., M. K. Hudson, W. Lotko, and R. Bergmann, Decay of ion beam driven acoustic waves into ion holes, *Geophys. Res. Lett.*, *18*, 1675-1678, 1991.

Gurnett, D. A. and R. R. Anderson, The kilometric radio emission spectrum: Relationship to auroral acceleration processes, in *Physics of Auroral Arc Formation*, edited by S.-I. Akasofu and J. R. Kan, *Geophys. Monogr. Ser.*, vol. 25, pp. 341-350, AGU, Washington, D.C., 1981.

Muschietti, L., R. E. Ergun, I. Roth, and C. W. Carlson, Phase-space electron holes along magnetic field lines, *Geophys. Res. Lett.*, *26*, 1093-1096, 1999. (Correction, *26*, 1689, 1999.)

Omura, Y., H. Matsumoto, and H. Kojima, Electron beam instability as generation mechanism of electrostatic electrostatic solitary waves in the magnetotail, *J. Geophys. Res.*, *101*, 2685-2697, 1996.

Pottelette, R., R. A. Treumann, G. Holmgren, N. Dubouloz, and M. Malingre, Acceleration and radiation from auroral cavitons, in *Auroral Plasma Dynamics*, edited by R. L. Lysak, *Geophys. Monogr. Ser.*, vol. 75, pp. 253-265, Washington, D.C., 1993.

Pottelette, R., R. E. Ergun, R. A. Treumann, M. Berthomier, C. W. Carlson, J. P. McFadden, and I. Roth, Modulated electron acoustic waves in auroral density cavities: FAST Observations, *Geophys. Res. Lett.*, *26*, 2629-2632, 1999.

Pritchett, P. L., Relativistic dispersion, the cyclotron maser instability, and auroral kilometric radiation, *J. Geophys. Res.*, *89*, 8957-8970, 1984.

Pritchett, P. L. and R. J. Strangeway, A simulation study of kilometric radiation generation along an auroral field line, *J. Geophys. Res.*, *90*, 9650-9662, 1985.

Pritchett, P. L., R. J. Strangeway, C. W. Carlson, R. E. Ergun, J. P. McFadden, and G. T. Delory, Free energy source and frequency bandwith for the auroral kilometric radiation, *J. Geophys. Res.*, *104*, 10,317-10,326, 1999.

Strangeway, R. J., Wave dispersion and ray propagation in a weakly relativistic electron plasma: Implications for the generation of auroral kilometric radiation, *J. Geophys. Res.*, *90*, 9675-9687, 1985.

Strangeway, R. J., On the applicability of relativistic dispersion to auroral zone electron distributions, *J. Geophys. Res.*, *91*, 3152-3166, 1986.

Strangeway, R. J., et al., FAST observations of VLF waves in the auroral zone: Evidence of very low plasma densities, *Geophys. Res. Lett.*, *25*, 2065-2068, 1998.

Strangeway, R. J, R. E. Ergun, C. W. Carlson, J. P. McFadden, G. T. Delory, and P. L. Pritchett, Accelerated electrons as the source of auroral kilometric radiation, *Phys. Chem. Earth*, in press, 2000.

Tokar, R. L., and S. P. Gary, Electrostatic hiss and the beam driven electron acoustic instability in the dayside polar cusp, *Geophys. Res. Lett.*, *11*, 1180-1183, 1984.

Winglee, R. M., and P. L. Pritchett, The generation of low-frequency electrostatic waves in association with Auroral Kilometric Radiation, *J. Geophys. Res.*, *91*, 13,531-13,541, 1986.

Wu, C. S., and L. C. Lee, A theory of terrestrial kilometric radiation, *Astrophys. J.*, *230*, 621-626, 1979.

M. Berthomier, Space Sciences Laboratory, The University of California at Berkeley, Berkeley, CA 94720-7450, USA. (matthieu@ssl.berkeley.edu)

R. Pottelette, CETP, 4 avenue de Neptune, F-94107 Saint Maur des Fosses, France. (raymond.pottelette@cetp.ipsl.fr)

R. A. Treumann, Centre for Interdisciplinary Plasma Science, Max-Planck-Institute for extraterrestrial Physics, Karl-Schwarzschild-Strasse 1, D-85748 Garching, Germany. (tre@mpe.mpg.de)

(Received March 24, 2000; revised August 23, 2000; accepted August 23, 2000.)